J|A|C|S
ARTICLES
Published on Web 06/08/2004

Effect of Adlayer Structure on the Host−Guest Recognition between Calcium and Crown-Ether-Substituted Phthalocyanine Arrays on Au Single-Crystal Surfaces

Soichiro Yoshimoto,[†] Koji Suto,[†] Akinori Tada,[†] Nagao Kobayashi,*[,‡] and Kingo Itaya*[,†,§]

Contribution from the Department of Applied Chemistry, Graduate School of Engineering, Tohoku University, Aoba-yama 04, Sendai 980-8579, Japan, Department of Chemistry, Graduate School of Science, Tohoku University, Sendai 980-8578, Japan, and Core Research Evolutional Science and Technology organized (CREST) by Japan Science and Technology Agency (JST), Kawaguchi Center Building, 4-1-8 Honcho, Kawaguchi, Saitama 332-0012, Japan

Received March 3, 2004; E-mail: itaya@atom.che.tohoku.ac.jp; nagaok@mail.tains.tohoku.ac.jp

Abstract: Adlayers of 15-crown-5-ether-substituted cobalt(II) phthalocyanine (CoCRPc) were prepared by immersion of either Au(111) or Au(100) substrate into benzene−ethanol (9:1 v/v) mixed solutions containing CoCRPc. In situ STM imaging was carried out after transferring the CoCRPc-modified Au crystals into aqueous $HClO_4$ solution. The packing arrangement of the CoCRPc array on Au(111) was determined to be $p(8 \times 4\sqrt{3}R - 30°)$, and the internal structure was clearly observed by high-resolution STM. Two adlayer structures of CoCRPc, (8×9) and $(4\sqrt{5} \times 4\sqrt{5})R26.7°$, were found on the Au(100)−(1×1) terrace. In the presence of 1 mM Ca^{2+}, two Ca^{2+} ions were trapped in two diagonally located 15-crown-5-ether moieties of each CoCRPc molecule on Au(111), whereas encapsulation of Ca^{2+} ions was not seen in the CoCRPc arrays on the Au(100)−(1×1) surface. The present study demonstrates that the relationship between crown moieties of CRPc and the underlying Au lattice is important in the trapping of Ca^{2+} ions in crown rings.

Introduction

Metallophthalocyanines (MPcs) have been extensively studied in the areas of gas sensors,[1,2] liquid crystals,[1] organic semiconductors,[1] electrocatalysis,[3] and field effect transistors (FET).[1] The formation and characterization of ordered adlayers of MPcs at interfaces are important from both academic and industrial standpoints. Among the various MPc structures that can be obtained via peripheral substitution, crown-ether-substituted Pc derivatives have the unique property of complexing with various alkali and inorganic cations.[1] CuPc substituted with four 15-crown-5-ether molecules (CuCRPc) was synthesized independently by three different groups of investigators at about the same time in 1986.[4−6] Subsequently, CoCRPc, NiCRPc, and ZnCRPc were synthesized by Kobayashi and Lever.[4a] In a mixed solvent of chloroform and methanol, these metalloCRPcs form eclipsed cofacial dimers via a two-step, three-stage process upon addition of cations such as K^+ [4−6] and Ca^{2+}.[4a] Nolte and co-workers showed that K^+, Rb^+, and Cs^+ complexes of 18-crown-6-ether-substituted H_2Pc possess electrical conductivities 2−3 orders of magnitude higher than those of Pcs without crown-ether moieties because of the formation of a stacking arrangement.[2] It was also reported that an 18-crown-6-ether-substituted H_2Pc derivative formed a supermolecular chiral fiber upon addition of K^+.[7]

Recently, scanning tunneling microscopy (STM) has been widely accepted as a powerful tool for understanding the structure of adlayers of molecules in solution.[8−11] The adlayer of H_2Pc molecules functionalized by four dibenzocrown-ether rings with enantiomerically pure (*S*)-3,7-dimethyloctyl chains was prepared on HOPG from a mixed organic solution, and it was observed in ambient conditions by STM.[12] Recently, Kunitake and co-workers prepared Langmuir films of both K^+-free and K^+-included dibenzo-18-crown-6 molecules.[13] They transferred the films onto Au(111) and directly observed by

[†] Department of Applied Chemistry, Tohoku University.
[‡] Department of Chemistry, Tohoku University.
[§] CREST.

(1) Guillaud, G.; Simon, J.; Germain, J. P. *Coord. Chem. Rev.* **1998**, *178−180*, 1433.
(2) Wright, J. D.; Roisin, P.; Rigby, G. P.; Nolte, R. J. M.; Cook, M. J.; Thorpe, S. C. *Sens. Actuators, B* **1993**, *13−14*, 276.
(3) Collman, J. P.; Wagenknecht, P. S.; Hutchison, J. E. *Angew. Chem., Int. Ed. Engl.* **1994**, *33*, 1537 and references therein.
(4) Koray, A. R.; Ahsen, V.; Bekâroğlu, Ö. *J. Chem. Soc., Chem. Commun.* **1986**, 932.
(5) (a) Kobayashi, N.; Nishiyama, Y. *J. Chem. Soc., Chem. Commun.* **1986**, 1462. (b) Kobayashi, N.; Lever, A. B. P. *J. Am. Chem. Soc.* **1987**, *109*, 7433. (c) Kobayashi, N. *Coord. Chem. Rev.* **2002**, *227*, 129.
(6) (a) Hendriks, R.; Sielecken, O. E.; Drenth, W.; Nolte, R. J. M. *J. Chem. Soc., Chem. Commun.* **1986**, 1464. (b) Sielecken, O. E.; van Tilborg, M. M.; Roks, M. F. M.; Hendriks, R.; Drenth, W.; Nolte, R. J. M. *J. Am. Chem. Soc.* **1987**, *109*, 4261.
(7) Engelkamp, H.; Middelbeek, S.; Nolte, R. J. M. *Science* **1999**, *284*, 785.
(8) Gewirth, A. A.; Niece, B. K. *Chem. Rev.* **1997**, *97*, 1129.
(9) Itaya, K. *Prog. Surf. Sci.* **1998**, *58*, 121.
(10) Kolb, D. M. *Angew. Chem., Int. Ed.* **2001**, *40*, 1162.
(11) Magnussen, O. M. *Chem. Rev.* **2002**, *102*, 679.
(12) Samorf, P.; Engelkamp, H.; Witte, P.; Rowan, A. E.; Nolte, R. J. M.; Rabe, J. P. *Angew. Chem., Int. Ed.* **2001**, *40*, 2348.
(13) Ohira, A.; Sakata, M.; Hirayama, C.; Kunitake, M. *Org. Biomol. Chem.* **2003**, *1*, 251.

10.1021/ja048760n CCC: $27.50

Chart 1. Chemical Formula of CoCRPc

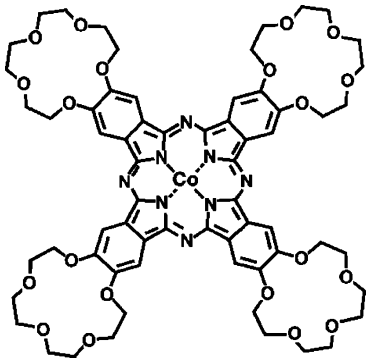

STM the difference in appearance of the two separately prepared adlayers in $HClO_4$ solution. However, to our knowledge, the inclusion of alkali metal ions in crown ethers on electrodes in solution has not been directly observed by in situ STM.

Thus, it is important to understand host−guest recognition at the electrochemical interface for designing a functional electrode with high selectivity. Recently, we reported that, of the four crown-ether moieties of the CoCRPc array on the Au(111) surface, only two crown-ether voids at diagonal positions trap two Ca^{2+} ions, where the location of the void centers exactly matches that of the hollows surrounded by three gold atoms.[14]

To obtain precise details on the host−guest recognition of calcium ions between the adlayer of CoCRPc and the underlying Au lattice, we have prepared CoCRPc (see Chart 1) arrays on both Au(111) and Au(100) surfaces in an organic solvent in the same manner as was used previously for the preparation of the adlayers of coronene,[15] fullerene monomer C_{60} and fullerene dimer C_{120},[16] 5,10,15,20-tetraphenyl-21*H*,23*H*-porphine cobalt(II) (CoTPP),[17] CoPc,[18] CoP,[19] and CoOEP.[19] Direct observation of the inclusion of Ca^{2+} into the crown-ether moieties was carried out in 0.05 M $HClO_4$ containing 1 mM Ca^{2+} by using in situ STM. The positional relationship between the crown rings in each CoCRPc molecule and the Au lattice was clearly determined by high-resolution STM images obtained in the present study.

Experimental Section

The CoCRPc used in our previous work[5] was recrystallized from chloroform−methanol. The Au(111) and Au(100) electrodes were prepared by the Clavilier method.[20] The aligned gold single-crystal bead was cut and polished successively with finer grades of alumina, and the electrode was then annealed in hydrogen flame at ca. 950 °C for at least 12 h in an electric furnace to remove mechanical damages. The Au(111)−(1 × 1) and Au(100)−(1 × 1) surfaces were obtained by quenching the Au electrode in ultrapure water saturated with hydrogen. Adlayers of CoCRPc were formed by immersing Au substrates for 5 min in a benzene−ethanol (9:1 v/v) mixed solution saturated with CoCRPc.[14] The CoCRPc-modified electrode was then rinsed with ultrapure water and transferred into an electrochemical or STM cell.

The aqueous $HClO_4$ solution was prepared from ultrapure grade $HClO_4$ (Cica-Merck) and ultrapure water (Milli-Q; ≥18.2 MΩ cm). Benzene (Kanto Chemical Co.; spectroscopy grade), ethanol (Kanto Chemical Co.; spectroscopy grade), $Ca(ClO_4)_2{\cdot}4H_2O$ (Aldrich 99%), and $KClO_4$ (Kanto Chemical Co.) were used without further purification.

Cyclic voltammetry was carried out at 20 °C using a potentiostat (HOKUTO HAB-151, Tokyo) with the hanging meniscus method in a three-compartment electrochemical cell under N_2 atmosphere. Electrochemical STM measurements were performed via a Nanoscope E (Digital Instruments, Santa Barbara, CA) with a tungsten tip etched in 1 M KOH. To minimize residual faradic currents, the tungsten tips were coated with nail polish. STM images were taken in the constant-current mode with a high-resolution scanner (HD-0.5I). All potentials are referred to the reversible hydrogen electrode (RHE). One of either the (111) or the (100) facet on the gold single-crystal bead was used as the substrate for electrochemical STM.[14−19] The CV and STM measurements of the CoCRPc adlayers were carried out in 0.05 M $HClO_4$. Complexation between CoCRPc and Ca^{2+} was allowed to proceed in 0.05 M $HClO_4$ containing ca. 1 mM Ca^{2+} ions.

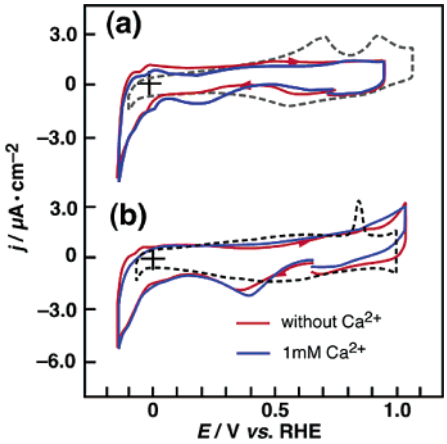

Figure 1. Typical cyclic voltammograms of bare (dashed line) and CoCRPc-modified Au(111) (a) and Au(100) (b) electrodes in 0.05 M $HClO_4$ in the absence (red lines) and presence (blue lines) of 1 mM Ca^{2+}. The CoCRPc adlayer was formed by immersing into either Au(111) or Au(100) substrate for 5 min in a benzene−ethanol mixed (9:1 v/v) solution saturated with CoCRPc. The potential scan rate was 20 mV s^{-1}.

Results and Discussion

Voltammetry. The Au single-crystal electrodes prepared by the procedure described above were examined in pure 0.1 M $HClO_4$ to identify each Au surface.[21] After the identification of the Au(111) and Au(100) single crystal was completed, the CV profile of each Au single-crystal electrode immersed in pure benzene for 10−60 s and rinsed with ultrapure water was essentially the same as that observed on a clean Au single-crystal electrode.[15] This result indicates that benzene adsorption onto Au(111) and Au(100) surfaces is so weak that benzene might be easily desorbed by rinsing with ultrapure water under the present conditions. Figure 1 shows typical CVs at bare (dashed lines) and CoCRPc-modified (red line) Au(111) electrodes in 0.05 M $HClO_4$, recorded at a scan rate of 20 mV s^{-1}. The voltammogram for the bare Au(111) in Figure 1a in the double-

(14) Yoshimoto, S.; Suto, K.; Itaya, K.; Kobayashi, N. *Chem. Commun.* **2003**, 2174.
(15) (a) Yoshimoto, S.; Narita, R.; Itaya, K. *Chem. Lett.* **2002**, 356. (b) Yoshimoto, S.; Narita, R.; Wakisaka, M.; Itaya, K. *J. Electroanal. Chem.* **2002**, *532*, 331.
(16) (a) Yoshimoto, S.; Narita, R.; Tsutsumi, E.; Matsumoto, M.; Itaya, K.; Ito, O.; Fujiwara, K.; Murata, Y.; Komatsu, K. *Langmuir* **2002**, *18*, 8518. (b) Matsumoto, M.; Inukai, J.; Tsutsumi, E.; Yoshimoto, S.; Itaya, K.; Ito, O.; Fujiwara, K.; Murata, M.; Murata, Y.; Komatsu, K. *Langmuir* **2004**, *20*, 1245.
(17) Yoshimoto, S.; Tada, A.; Suto, K.; Narita, R.; Itaya, K. *Langmuir* **2003**, *19*, 672.
(18) Yoshimoto, S.; Tada, A.; Suto, K.; Itaya, K. *J. Phys. Chem. B* **2003**, *107*, 5836.
(19) Yoshimoto, S.; Inukai, J.; Tada, A.; Abe, T.; Morimoto, T.; Osuka, A.; Furuta, H.; Itaya, K. *J. Phys. Chem. B* **2004**, *108*, 1948.
(20) Clavilier, J.; Faure, R.; Guinet, G.; Durand, R. *J. Electroanal. Chem.* **1980**, *107*, 205.
(21) (a) Angerstein-Kozlowska, H.; Conway, B. E.; Hamelin, A.; Stoicoviciu, L. *J. Electroanal. Chem.* **1987**, *228*, 429. (b) Hamelin, A. *J. Electroanal. Chem.* **1996**, *407*, 1.

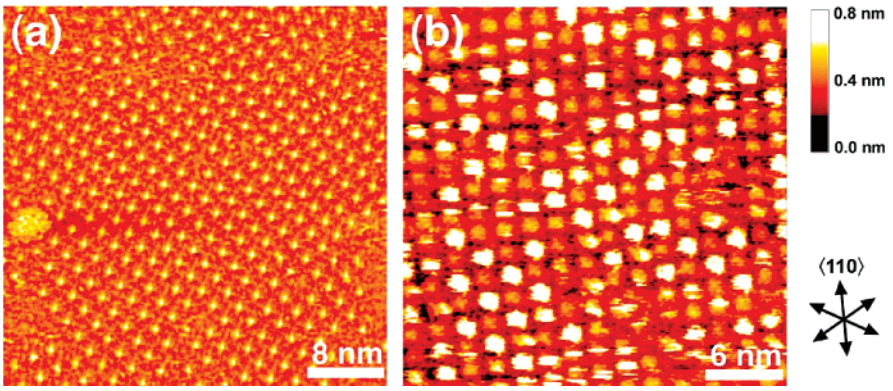

Figure 2. Typical large-scale STM images, acquired at 0.85 V vs RHE, of CoCRPc arrays on Au(111) in 0.05 M $HClO_4$ prepared in a benzene−ethanol (9:1 v/v) mixed solution containing CoCRPc. The immersion time was 5 min (a) and 7 min (b). The tip potential was 0.45 V. The tunneling currents were 2.0 nA (a) and 0.75 nA (b), respectively. The set of three arrows indicates the lattice directions of Au(111) substrate.

layer potential region is identical to that reported previously.[15b] For the electrode modified with CoCRPc, the electrode potential was scanned negatively from 0.9 V. A slight increase in cathodic current was observed at ca. 0.25 V. As described in our previous paper, the current for the reduction of Co(III) to Co(II) was observed at 0.22 V during the cathodic scan on the CoCRPc-modified Au(111) electrode.[18] According to the reports by Murray's group, on Au electrode modified with a CoTPP derivative having four thiol moieties, 5,10,15,20-tetrakis(*o*-(2-mercaptoethoxy)phenyl)porphyrin (Co(*o*-TMEPP), exhibited a redox wave originating from the Co(III/II) couple at ca. 0.15 V vs SCE in 1 M $HClO_4$ at a scan rate of 50 mV s^{-1}.[22] Even in a nominally degassed acidic solution, Murray and co-workers found that residual oxygen fully oxidized the Co(II) (*o*-TMEPP) monolayer formed on Au within 10 s.[22] In our case, the oxidation to Co(III) probably took place on the CoCRPc-adsorbed Au(111) electrode at the OCP in 0.05 M $HClO_4$, because the electrode was transferred into the electrochemical cell after washing with undegassed ultrapure water. The increase in cathodic current observed between 0.25 and 0 V might be due to the reduction of Co(III) to Co(II). The abrupt increase in cathodic current at 0 V is probably due to the desorption of CoCRPc and the evolution of H_2. In the presence of 1 mM Ca^{2+}, a nearly identical CV was obtained at the CoCRPc-modified Au(111) electrode. The CV profiles of the CoCRPc-modified Au(100) electrode obtained in the same manner are shown in Figure 1b. A small cathodic peak was seen at 0.35 V. The cathodic peak observed between 0.45 and 0.2 V is likely due to the reduction of Co(III) to Co(II). A clear difference in CV profile was observed between the Au(111) and Au(100) electrodes, while normal CoPc without crown units showed no difference in the reduction potential of Co(III) to Co(II) between Au(111) and Au(100), as shown in our previous papers.[17,23] We also examined the electrochemical reduction of O_2 at the CoCRPc-modified Au(111) and Au(100) electrodes to determine the reduction potential of Co(III) to Co(II). The O_2 reductions at the CoCRPc-modified Au(111) and Au(100) electrodes commenced at the same potentials as those for the Co(III) to Co(II) reduction under N_2 atmosphere, that is, 0.15 and 0.35 V, respectively (not shown). The reason the reduction potential of Co(III) to Co(II) was different on Au(111) and on Au(100) is unclear, but it might be attributable to the difference in potential of zero charge (pzc) for Au(111) and Au(100).[24]

In Situ STM. (1) CoCRPc on Au(111). Figure 2a shows a typical STM image of a CoCRPc adlayer on Au(111) obtained at 0.85 V in 0.05 M $HClO_4$, after the CoCRPc adlayer was prepared by immersing the Au(111) electrode for 5 min into a benzene−ethanol (9:1 v/v) mixed solution saturated with CoCRPc. Highly ordered molecular arrays of CoCRPc were observed consistently. In the STM image acquired in an area of 40 × 40 nm^2, individual CoCRPc molecules can be clearly recognized with an equal brightness, indicating the formation of a monolayer. In our previous study on the adlayers of CoTPP, CoPc, and CoOEP, we observed a modulation caused by reconstruction of Au(111) under the molecular layer, whereas reconstructed rows of the Au(111) substrate were not found under the CoCRPc molecular layer in the present study. The molecular rows of bright spots with flat-lying orientation are seen to cross each other at an angle of 90° within an experimental error of ±3°. The increase of the modification time revealed the formation of CoCRPc dimers. For example, the STM image shown in Figure 2b was obtained when the immersion time was 7 min. In this STM image, acquired in an area of 30 × 30 nm^2, individual CoCRPc molecules can be recognized as bright spots with a rectangular lattice. The brighter spots in Figure 2b were found to be higher in elevation than the darker spots by ca. 0.42 nm, which corresponds to the thickness of a single layer. Thus, the brighter spots are identified as the CoCRPc in the second layer. It is clearly seen in the image that CoCRPc in the second layer is adsorbed on top of CoCRPc in the first layer.

Figure 3a shows a typical plan view of a high-resolution STM image acquired in an area of 9 × 9 nm^2. It is clear that the CoCRPc molecules formed a well-ordered adlayer on Au(111). In addition to the information concerning the symmetry and the structure of CoCRPc arrays, this STM image reveals a great deal of information concerning the internal molecular structure. The shape of the observed features in the image is reminiscent of the molecular structure of CoCRPc. Each molecule can be seen as propeller-shaped with the brightest spot at the center, with four additional bright rings at the corners of each CoCRPc

(22) Postlethwaite, T. A.; Hutchison, J. E.; Hathcock, K. W.; Murray, R. W. *Langmuir* **1995**, *11*, 4109.
(23) Yoshimoto, S.; Tada, A.; Suto, K.; Yau, S.-L.; Itaya, K. *Langmuir* **2004**, *20*, 3159.
(24) (a) Kolb, D. M.; Schneider, J. *Electrochim. Acta* **1986**, *31*, 929. (b) *Structure of Electrified Interfaces*; Lipkowski, J., Ross, P. N., Eds.; Wiley−VCH: New York, 1993.

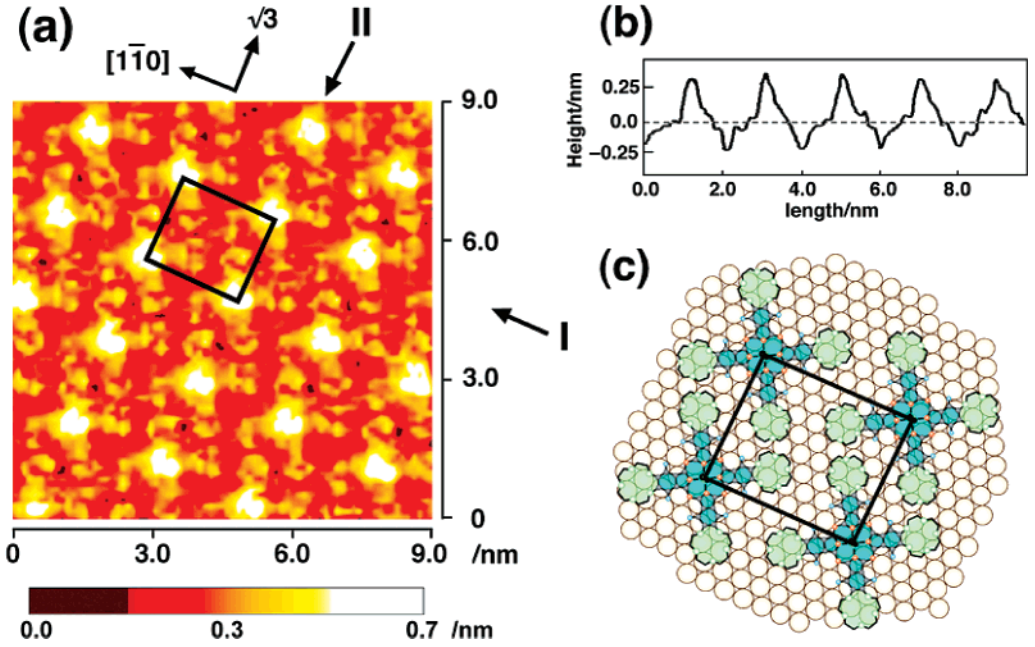

Figure 3. High-resolution (9×9 nm^2) STM image (a) and cross-sectional profile aligned to the direction of arrow II (b) of CoCRPc arrays on Au(111) surface in 0.05 M $HClO_4$, acquired at 0.85 V vs RHE. Tip potential and tunneling current were 0.45 V and 1.0 nA, respectively. Although there is no direct evidence that corroborates the location and orientation of CoCRPc molecules in relation to the atomic arrangement of underlying Au(111), the model for the CoCRPc adlayer on the Au(111) surface is superimposed as a $p(8 \times 4\sqrt{3}R - 30°)$ unit cell (c).

molecule. All molecules are oriented in the same direction on Au(111). The corners of each CoCRPc molecule are arranged in a side-by-side configuration; that is, crown rings of nearest neighbor molecules are closely positioned with respect to each other. As reported by Hipps' group in UHV[25,26] and by our group in solution,[17−19] the center of each CoCRPc molecule appears as the brightest spot in the STM image because of the tunneling being mediated by a half filled d_{z^2} orbital between the Au surface and the tip. However, at 0.8 V, the central Co ion is in the state of Co(III) formed by the electrochemical oxidation (Figure 1b). Because the d_{z^2} orbital should be empty in this oxidation state, another mechanism must be taken into consideration to explain the tunneling at the central Co(III)-CRPc. It is generally known that the Co(III) porphyrin is unstable and, to make it more stable, the addition of an axial ligand, such as O_2, is necessary.[27a] Because our STM measurements were carried out in solution containing air, it is feasible that O_2 molecules dissolved in solution were eventually attached to Co(III) ions to stabilize the Co(III)CRPc molecule. According to a previous paper, the stronger σ-donating axial ligands lead to the smaller Co hyperfine coupling, promoting the localization of π-electrons on the oxygen.[27a] This π orbital might act as a new tunneling pathway, which could increase the tunneling current at the central position of Co(III)CRPc. Actually, as shown in Figure 3b, the height value of each central spot was measured to be ca. 0.45 nm from the cross-sectional profile aligned to the direction indicated by arrow II. This value is higher than that obtained in the presence of O_2 (2×10^{-7} Torr) in UHV by Hipps' group (0.3 nm).[25b] In aqueous solution, the adsorption of O_2 might be promoted by water molecules, particularly because it is known that the O_2 molecule coordinates to the Co(III) porphyrin as a super oxide anion.[27a] Furthermore, water molecules might coordinate with Co(III)Pc in an aqueous solution, because the complexes such as $[CoTPP(H_2O)_2]ClO_4$ or $[CoOEP(H_2O)_2]ClO_4$ are also known.[27b] On the basis of the cross-sectional profile, the distance between the centers of diagonally located spots in the molecule was found to be 2.02 $\pm$ 0.05 nm, which is in good agreement with the chemical structure shown in Chart 1. Comparison between the molecular arrays and the step lines running along the Au lattice reveals that the molecular rows are aligned along the atomic row and the $\sqrt{3}$ directions. The unit cell is superimposed as a rectangular lattice in Figure 3a. The intermolecular spacings between CoCRPc molecules aligned in the [1$\bar{1}$0] (arrow I) and $\sqrt{3}$ (arrow II) directions were found to be 2.34 $\pm$ 0.07 and 2.03 $\pm$ 0.05 nm, respectively, which correspond to 8 and $4\sqrt{3}$ times the Au lattice constant. Therefore, the commensurate $p(8 \times 4\sqrt{3}R - 30°)$ structure is assigned to the unit cell. Those observed distances are slightly larger than the lattice parameters of the bulk crystal structure, 2.05 and 1.8 nm, in a rectangular lattice.[28] Highly ordered CoCRPc arrays with the oblique structure were consistently observed in the potential range between 0.4 and 0.9 V.

A structural model of $p(8 \times 4\sqrt{3}R - 30°)$ is proposed in Figure 3c. The unit cell is drawn with solid lines. To determine the adsorption sites, we considered the effect of moving the unit cell in parallel directions with respect to the Au(111)−(1 $\times$ 1) substrate and found that the geometry drawn in Figure 3c

(25) (a) Lu, X.; Hipps, K. W.; Wang, X. D.; Mazur, U. *J. Am. Chem. Soc.* **1996**, *118*, 7197. (b) Hipps, K. W.; Lu, X.; Wang, X. D.; Mazur, U. *J. Phys. Chem.* **1996**, *100*, 11207. (c) Lu, X.; Hipps, K. W. *J. Phys. Chem. B* **1997**, *101*, 5391. (d) Barlow, D. E.; Hipps, K. W. *J. Phys. Chem. B* **2000**, *104*, 5993.

(26) (a) Scudiero, L.; Barlow, D. E.; Hipps, K. W. *J. Phys. Chem. B* **2000**, *104*, 11899. (b) Scudiero, L.; Barlow, D. E.; Mazur, U.; Hipps, K. W. *J. Am. Chem. Soc.* **2001**, *123*, 4073.

(27) (a) *Porphyrins and Metalloporphyrins*; Smith, K. M., Ed.; Elsevier/North-Holland Biomedical Press: Amsterdam, 1976. (b) Brothers, P. J. In *Advances in Organometallic Chemistry*; Stone, F. G. A., West, R., Eds.; Academic Press: San Diego, CA, 2000; Vol. 46, pp 223−321.

(28) Sirlin, C.; Bosio, L.; Simon, J.; Ahsen, V.; Yilmazer, E.; Bekâroğlu, Ö. *Chem. Phys. Lett.* **1987**, *139*, 362.

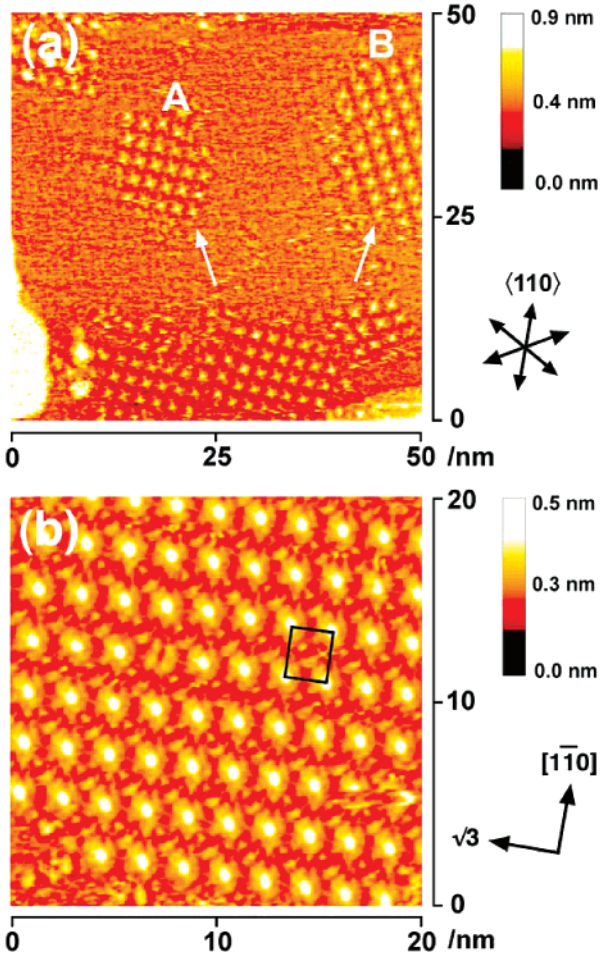

Figure 4. Large-scale (50 × 50 nm^2) (a) and higher-resolution (20 × 20 nm^2) (b) STM images of CoCRPc adlayer on Au(111) surface in 0.05 M $HClO_4$ in the presence of 1 mM Ca^{2+} acquired at 0.85 V (a) and 0.8 V (b). The tip potential and tunneling current were 0.44 V and 1.8 nA for (a) and 0.35 V and 5.0 nA for (b), respectively.

gives the most symmetric configuration. In this model, the central Co ions and all of the crown-ether moieties are situated at 2-fold bridge sites. In this configuration, each molecule on Au(111) has a 2-fold symmetry.

After the formation of a well-defined adlayer of CoCRPc was confirmed in pure 0.05 M $HClO_4$ by STM, a 0.05 M $HClO_4$ solution containing 10 mM Ca^{2+} was added dropwise into the electrochemical STM cell. The concentration of Ca^{2+} in the STM cell was ca. 1 mM. Figure 4 shows STM images of a CoCRPc adlayer formed on the Au(111) surface after adding Ca^{2+} ions. A large-scale STM image with several domains on the terrace is shown in Figure 4a. Although the STM image was obtained for a submonolayer of CoCRPc in the presence of Ca^{2+}, it provides important information about the trapping of Ca^{2+} ions. The molecular rows between two domains A and B crossed each other at an angle of ca. 60°. Molecular rows in both domains are aligned along either the atomic row or the $\sqrt{3}$ direction of the Au(111) lattice, but the relationship between the two domains is such that they constitute a set of rotational domains. Furthermore, each molecule in both domains was diagonally bright along the directions indicated by the white arrows, but careful inspection shows that there is a difference between the molecules in domains A and B. The vertical direction on the left edge of each molecule was bright in domain A, whereas that on the right edge was bright in domain B. These features are strongly associated with the complexation between Ca^{2+} ions and crown-ether moieties in the CoCRPc adlayer on Au(111). Note that the STM image in Figure 4a was obtained under conditions similar to those in Figure 2a. As shown in Figure 4b, the close-up view of one of the two domains acquired in an area of 20 × 20 nm^2 revealed highly ordered arrays of CoCRPc molecules on the terrace in the presence of 1 mM Ca^{2+}. It is clearly seen in this image that all molecules are oriented in the same direction on Au(111). The unit cell is superimposed as a rectangular lattice in Figure 4b, which is identical to that obtained in $HClO_4$ solution without Ca^{2+}, $p(8 \times 4\sqrt{3}R - 30°)$.

A high-resolution STM image is shown in Figure 5a. Each CoCRPc molecule exhibits a characteristic shape with the brightest spot at the center, except for the molecule located on the left of the center of the image, in which the central metal appears to be missing. In the absence of Ca^{2+}, four additional spots were observed at the corners, whereas in the presence of Ca^{2+}, only two additional bright spots were observed at diagonal positions with respect to the Pc ligand, as marked by two circles in Figure 5a, as a result of encapsulation of two Ca^{2+} ions by crown-ether rings. The distance between two additional bright spots was about 2.03 ± 0.07 nm, corresponding to that between two crown-ether moieties in one CoCRPc molecule. It is known that STM images in general vary with the experimental conditions such as magnitudes of tunneling current and bias voltage. In our system, STM images were recorded under several imaging conditions. Although the images were particularly affected by the tunneling conditions, STM images between those obtained in the absence and the presence of Ca^{2+} were very clear (see Supporting Information). Therefore, we conclude that the STM image shown in Figure 5a resulted from the encapsulation of two Ca^{2+} ions into the opposite crown-ether moieties of the CoCRPc molecule.

A careful inspection of Figure 5a with Figure 3a reveals that the diagonal axis of each CoCRPc molecule is rotated anticlockwise by ca. 10°. The result seems to indicate that each CoCRPc molecule was slightly rotated upon trapping Ca^{2+} ions in the crown rings. A schematic model is presented in Figure 5b. In this model, central Co^{2+} ions are located at 2-fold bridge sites, but the diagonal axes of CoCRPc are rotated by ca. 10° with respect to the direction of the Au atomic row (Figure 5a). With this rotational angle, the centers of the two crown-ether moieties, which are shown in red, are situated at hcp and fcc 3-fold hollow sites, whereas the other two unoccupied moieties colored green are at near bridge sites. The rotation of molecules upon complexation with Ca^{2+} might have been caused by a change in interaction between the crown-ether moieties in neighboring molecules. It might also be possible that crown ethers with Ca^{2+} ions favor 3-fold sites, as depicted in the side view in Figure 5b. The distance between the Au lattice and crown moieties probably plays a significant role in the host−guest recognition. Further investigations are required to understand the cause of the rotation more clearly. It was noted that STM images obtained in the presence of 1 mM K^+ were identical to those obtained in pure $HClO_4$. The radii of Ca^{2+} and K^+ ions are 1.98 and 2.66 Å, respectively,[5b] whereas the size of the 15-crown-5-ether ring is estimated to be 1.7−2.2 Å.[5b] Thus, K^+ ion appears to be too large to be trapped in 15-

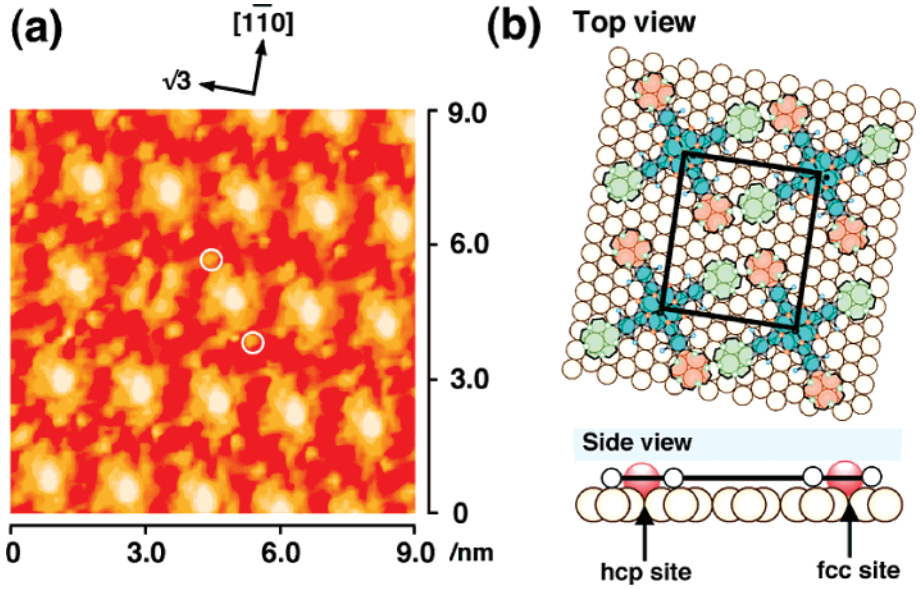

Figure 5. High-resolution STM image (9 × 9 nm^2) (a) and top and side models (b) of CoCRPc adlayer on Au(111) surface in 0.05 M $HClO_4$ containing 1 mM Ca^{2+}. The STM image was acquired at 0.8 V vs RHE. The tip potential and tunneling current were 0.35 V and 5.0 nA, respectively. The proposed structural model for an array of CoCRPc molecules complexed with Ca^{2+} on an Au(111)−(1 × 1) surface has a superimposed $p(8 \times 4\sqrt{3}R - 30°)$ unit cell, although there is no direct evidence supporting the location and orientation of CoCRPc molecules in relation to the atomic arrangement of the underlying Au(111).

crown-5-ether rings. These results indicate that the size of the ion is recognized by 15-crown-5-ether moieties located at the 3-fold hollow site.

(2) CoCRPc Array on Au(100). To obtain structural details on the effect of the crystallographic orientation of Au, the structure of a CoCRPc adlayer on Au(100) was further investigated in 0.05 M $HClO_4$ containing 1 mM Ca^{2+}. Figure 6a shows an STM image of CoCRPc arrays formed on Au(100)−(1 × 1) by immersion in a CoCRPc-saturated benzene−ethanol (9:1 v/v) mixed solution for 5 min, where the Au(100)−(1 × 1) was prepared by immediately quenching a freshly annealed Au(100) substrate in ultrapure water. The terrace was fully covered with CoCRPc arrays. However, we could also see some Au islands with a monatomic height formed by phase transition from (hex) to (1 × 1). In general, the Au(100) surface is known to form many Au islands due to the lifting of reconstruction which occurs immediately after quenching in ultrapure water.[29,30] Although we could discriminate individual CoCRPc molecules in an area of 75 × 75 nm^2, the domain size for the CoCRPc array on Au(100)−(1 × 1) was much smaller than that on Au(111)−(1 × 1) because of the formation of monatomic Au islands on the terrace. The difference in domain size might be due to the difference in interaction between CoCRPc and Au(111) and that between CoCRPc and Au(100). To overcome the difficulty of observing the adlayer, Au islands were allowed to diffuse by holding the electrode potential at 1.0 V for more than 20 min. We found wide atomically flat terraces after this electrochemical treatment. Figure 6b shows an STM image of CoCRPc arrays on Au(100)−(1 × 1) obtained at 0.75 V. Two different domains are seen, in which molecular rows were aligned to atomic and √5 directions. The molecular rows in domains A and B intersect each other at the boundary at an angle of 26° within an experimental error of ±3°. This result indicates that domains A and B are not rotational but different

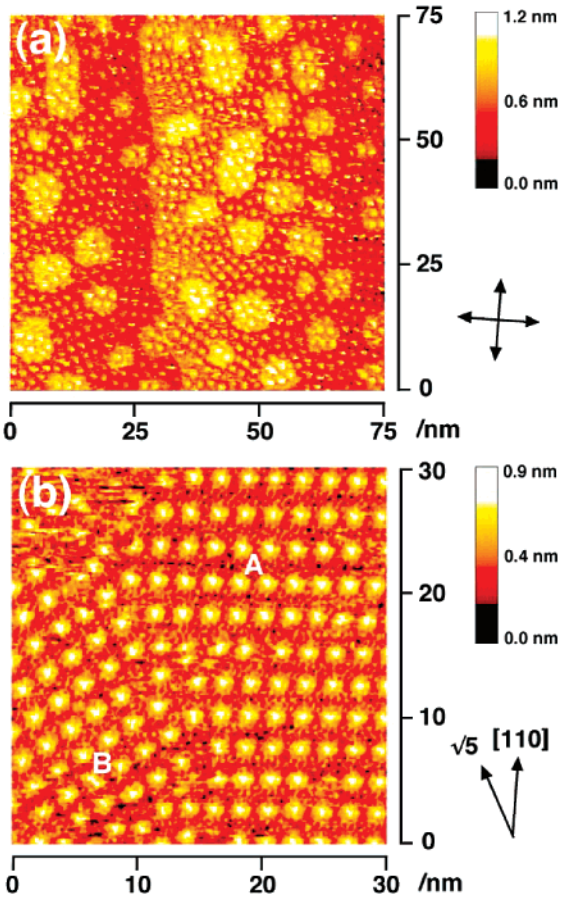

Figure 6. Large-scale (75 × 75 nm^2) STM image of the CoCRPc adlayer formed on the Au(100)−(1 × 1) surface in 0.05 M $HClO_4$ in the presence of 1 mM Ca^{2+}, acquired at 0.75 V vs RHE. The tip potential and tunneling current were 0.35 V and 1.5 nA, respectively. The two arrows indicate close-packed and √5 directions of the Au(100) substrate.

(29) (a) Magnussen, O. M.; Hotlos, J.; Behm, R. J.; Batina, N.; Kolb, D. M. *Surf. Sci.* **1993**, *296*, 310. (b) Gao, X.; Edens, G. J.; Hamelin, A.; Weaver, M. J. *Surf. Sci.* **1993**, *296*, 333.
(30) *Interfacial Electrochemistry*; Wieckowski, A., Ed.; Marcel Dekker, Inc: New York, 1999.

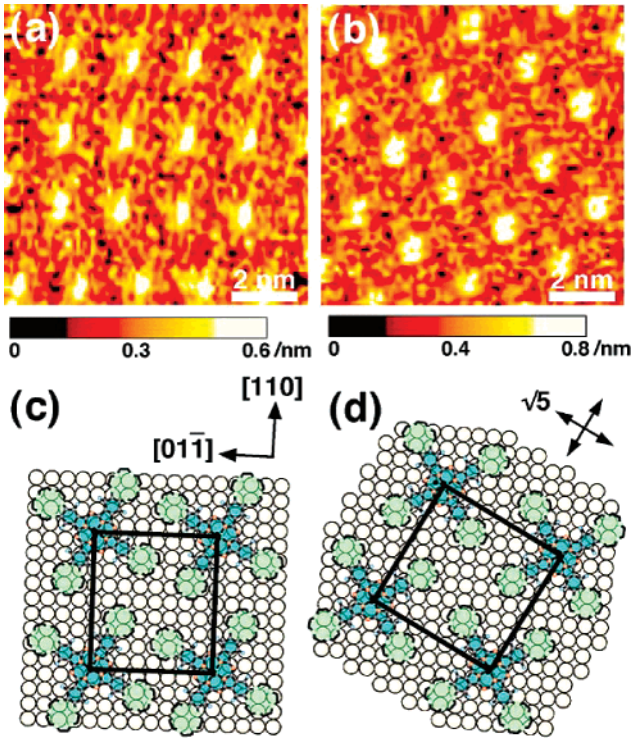

Figure 7. High-resolution STM images acquired at 0.75 V vs RHE (a and b) and models (c and d) of the CoCRPc adlayer formed on the Au(100)−(1 × 1) surface in 0.05 M $HClO_4$ in the presence of 1 mM Ca^{2+}. The tip potential was 0.35 V for both (a) and (b), while tunneling currents were 1.5 nA (a) and 2.25 nA (b), respectively. The set of two arrows indicates $\sqrt{5}$ directions of the Au(100) substrate. The proposed structural models for an array of CoCRPc on an Au(100)−(1 × 1) surface has superimposed (8 × 9) and (4$\sqrt{5}$ × 4$\sqrt{5}$)*R*26.7° unit cells, although there is no direct evidence corroborating the location and orientation of CoCRPc molecules in relation to the atomic arrangement of the underlying Au(100)−(1 × 1).

structural domains. In the potential range between 1.0 and 0.1 V, identical CoCRPc structures were observed on Au(100)−(1 × 1). At potentials more negative than 0 V, the ordered arrays of CoCRPc became unclear because of its high mobility on the Au(100) surface.

To understand the structural details, two high-resolution STM images of regions A and B in Figure 6b are shown in Figure 7a and b. While the adlayer of CoCRPc on Au(100)−(1 × 1) was exposed in a 0.05 M $HClO_4$ solution containing 1−2 mM Ca^{2+}, 15-crown-5-ether rings in each CoCRPc molecule are clearly seen in both STM images. These results show that Ca^{2+} ions are not complexed with the crown rings in the CoCRPc adlayer on Au(100)−(1 × 1). As shown in Figure 7a, the molecular rows are seen to be aligned to the Au lattice directions. Each molecule is also seen to be propeller-shaped with the brightest spot at the center, and four additional bright rings at the corners of each CoCRPc molecule. The corners of each CoCRPc molecule are also seen to be arranged in a side-by-side configuration, as was observed on Au(111). Intermolecular distances were estimated to be 2.33 ± 0.05 and 2.61 ± 0.07 nm in the [01$\bar{1}$] and [110] directions, respectively, which corresponds to 8 and 9 times the Au lattice constant. Therefore, the adlattice in domain A can be explained by a unit cell having an (8 × 9) structure, which was slightly larger than that on Au(111). In domain B, four crown-ether rings are also seen in each CoCRPc molecule. The intermolecular spacings between nearest neighbor molecules in domain B were found to be 2.59 ± 0.06 and 2.61 ± 0.07 nm in the $\sqrt{5}$ directions, respectively, which corresponds to 4$\sqrt{5}$ times the Au lattice constant. Proposed models for the STM images in Figure 7a and b are shown in Figure 7c and d, respectively. On the basis of the STM images in Figure 7a and b, we also determined the adsorption sites by moving the unit cell in parallel directions with respect to the Au(100)−(1 × 1) substrate. In both models, all 15-crown-5-ether moieties are situated not at non-4-fold hollow sites but at near 2-fold bridge sites when the central Co ion is positioned at 2-fold bridge sites. It is noteworthy that the image of the CoCRPc adlayer on Au(100)−(1 × 1) strongly depended upon the tunneling current. When the usual tunneling current of lower than 2 nA was used, the CoCRPc adlayer on Au(100)−(1 × 1) was clearly resolved as a well-defined chemical structure. When the scanning for the adlayer on the Au(100)−(1 × 1) surface was carried out with tunneling currents higher than 3 nA, the image of adsorbed CoCRPc molecules became gradually smaller in size with repeated scanning. The result indicates that CoCRPc molecules are ejected when strong tunneling currents are used and that the interaction between the CoCRPc molecule and Au(100) surface is not particularly strong.

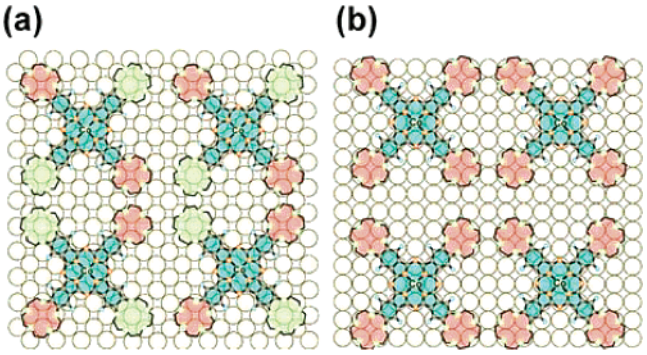

Figure 8. Possible models for the CoCRPc adlayer formed on the Au(100)−(1 × 1) surface.

Several models are conceivable for the complexation of CoCRPc with Ca^{2+} on the Au(100)−(1 × 1) lattice, as illustrated in Figure 8. For example, when the central Co of each CoCRPc molecule is situated at a 2-fold bridge site and those molecules are arranged in a side-by-side configuration aligned in the $\sqrt{2}$ direction as shown in Figure 8a, two diagonally positioned crown moieties should be located at 4-fold hollow sites of the Au(100) lattice, whereas the other diagonally positioned moieties are situated on the 2-fold bridge sites. In this case, the adsorption site of central Co ion is located at a different bridge site, and hence the Ca^{2+}-trapped positions in each CoCRPc molecule become Ca^{2+}-untrapped positions in the neighboring CoCRPc molecules. If the central Co ion is located at the on-top site and each molecule is aligned in the lattice direction of Au(100) as shown in Figure 8b, all crown moieties are situated at 4-fold hollow sites. However, such a configuration has never been seen on the Au(100)−(1 × 1) surface. These results indeed support the conclusion that the distance between the Au lattice and crown moieties plays a significant role in the host−guest recognition.

Conclusions

By immersing Au single-crystal substrates into benzene−ethanol (9:1 v/v) mixed solutions saturated with CoCRPc, we

succeeded in preparing well-defined adlayers of CoCRPc on both Au(111) and Au(100)−(1 × 1) surfaces and resolving, by high-resolution STM, their packing arrangement and the internal molecular structure of each CoCRPc molecule adsorbed on the Au(111) electrode in aqueous $HClO_4$. CoCRPc molecules formed a well-defined adlayer having a $p(8 \times 4\sqrt{3}R - 30°)$ oblique lattice on the Au(111) surface, whereas two adlattices of (8 × 9) and $(4\sqrt{5} \times 4\sqrt{5})R26.7°$ structures were found on Au(100)−(1 × 1). In the presence of Ca^{2+}, the CoCRPc adlayer on Au(111) trapped Ca^{2+} ions in two diagonally located 15-crown-5-ether moieties. The results of direct imaging of host−guest recognition of Ca^{2+} demonstrated that CoCRPc-modified Au(111) trapped two Ca^{2+} ions in 15-crown-5-ether moieties in each molecule, while CoCRPc-modified Au(100)−(1 × 1) did not encapsulate Ca^{2+} ions. Thus, the host−guest recognition of Ca^{2+} ions depends on the crystallographic orientation of Au. Our results suggest that precise control of adlayer structures plays a highly selective role for the guest molecule; that is, the relationship between the crown moieties and the underlying Au lattice is important.

Acknowledgment. This work was supported in part by CREST-JST, by the Ministry of Education, Culture, Sports, Science, and Technology, and by a Grant-in-Aid for the Center of Excellence (COE) Project, Giant Molecules and Complex Systems, 2004. We acknowledge Dr. Y. Okinaka for his assistance in writing this manuscript.

Supporting Information Available: STM images. This material is available free of charge via the Internet at http://pubs.acs.org.

JA048760N